Preparation of a neutral nitrogen allotrope hexanitrogen C_{2h}-N_6

https://doi.org/10.1038/s41586-025-09032-9

Received: 18 September 2024

Accepted: 16 April 2025

Published online: 11 June 2025

Open access

Check for updates

Weiyu Qian[1], Artur Mardyukov[1]✉ & Peter R. Schreiner[1]✉

Compounds consisting only of the element nitrogen (polynitrogens or nitrogen allotropes) are considered promising clean energy-storage materials owing to their immense energy content that is much higher than hydrogen, ammonia or hydrazine, which are in common use, and because they release only harmless nitrogen on decomposition[1]. However, their extreme instability poses a substantial synthetic challenge and no neutral molecular nitrogen allotrope beyond N_2 has been isolated[2,3]. Here we present the room-temperature preparation of molecular N_6 (hexanitrogen) through the gas-phase reaction of chlorine or bromine with silver azide, followed by trapping in argon matrices at 10 K. We also prepared neat N_6 as a film at liquid nitrogen temperature (77 K), further indicating its stability. Infrared and ultraviolet–visible (UV-Vis) spectroscopy, ^{15}N-isotope labelling and ab initio computations firmly support our findings. The preparation of a metastable molecular nitrogen allotrope beyond N_2 contributes to our fundamental scientific knowledge and possibly opens new opportunities for future energy-storage concepts.

Molecular nitrogen allotropes beyond N_2 are promising for the development of high-energy-density materials[4] because they release enormous energy on dissociation into gaseous N_2. As the main component of air, N_2 is inert, non-toxic and not a greenhouse contributor[5–7]. Unlike carbon, N_2 is the only nitrogen allotrope found in nature and strategies for synthesizing higher neutral molecular nitrogen allotropes are highly sought after[8–14]. However, they are deemed extremely unstable, especially when uncharged and with an even electron count[15]. Consequently, only two examples have been reported. The azide radical ($\bullet N_3$) (Fig. 1a) was identified in the gas phase through rotational spectroscopy in 1956 (refs. 16,17). In 2002, N_4 was detected by gas-phase neutralization-reionization mass spectrometry (NRMS); its structure has not been revealed[18]. The intermediacy of an N_6 species was tentatively suggested in 1970 in the decay of azide radicals in aqueous solution but no definitive spectroscopic evidence was provided[19].

There are many computations proposing molecular allotropes spanning from N_4 to N_{120}, including chains, rings and cages[7,20], most of which have low dissociation barriers into N_2. For example, hexazine (*cyc*-N_6, the nitrogen analogue of benzene) exhibits a computed barrier of only 4.2 kcal mol^{-1} for decomposition into three N_2 (ref. 21). Quantum mechanical tunnelling (QMT) effects could further reduce the lifetime of higher nitrogen allotropes, adding to their difficulty of preparation[22].

Although the pursuit of higher neutral molecular nitrogen allotropes is extremely challenging, several homonuclear polynitrogen ions have been isolated. The synthesis and characterization of $[N_5]^+[PnF_6]^-$ (Pn = As, Sb) salts with a bent pentanitrogen cation represents a milestone[23,24]. Christe et al. initially identified the *cyclo*–N_5^- anion using mass spectrometry in 2002 and 2003 (refs. 25,26) and Zheng et al. reported in 2017 the synthesis of a salt featuring the *cyclo*–N_5^- anion[27]. The synthesis of various metal pentazolates was achieved through the reaction of $[Na(H_2O)(N_5)]\bullet 2H_2O$ with metal salts[28,29].

In the realm of solid-state (non-molecular) structures, a breakthrough was the high-temperature (2,000 K), high-pressure (110 GPa) diamond-like solid-state cubic gauche nitrogen phase in which all atoms are connected by single bonds[30,31]. An aromatic cyclic hexazine N_6^{4-} was identified through solid-state X-ray diffraction of K_9N_{56} under pressures above 40 GPa and temperatures above 2,000 K (ref. 32). Greschner et al. predicted a new nitrogen molecular crystal comprising N_6 units with an open-chain structure stabilized by electrostatic interactions[33], in line with assessments for the molecular species[9].

In our analysis of the proposed molecular nitrogen allotropes, acyclic neutral N_6 (hexaaza-1,2,4,5-tetraene, hexanitrogen, diazide) stands out because N_2 moieties are not discernible (Fig. 1). The central N–N bond would lead to unproductive endothermic dissociation (ΔG_{298K} theor. +26.1 kcal mol^{-1}, vide infra) into two $\bullet N_3$. Furthermore, the computed dissociation barrier into three N_2 molecules of $\Delta G^{\ddagger}_{298K}$ = 14.8 kcal mol^{-1} makes N_6 a promising candidate for synthesis. Here we show that N_6 indeed can be prepared at room temperature through the reaction of Cl_2 or Br_2 with AgN_3 under reduced pressure, followed by cryogenic trapping[34]. The characterization was accomplished by infrared (including ^{15}N-isotope labelling) as well as UV-Vis spectroscopy and ab initio computations. We also demonstrate the preparation and stability of C_{2h}-symmetric N_6 (hereinafter referred to as N_6) in neat form as a film at the temperature of liquid nitrogen (77 K).

Synthesis of N_6

As AgN_3 is an excellent reagent for the synthesis of polyazides[35] and halogen azides both in the gas phase[36] and in solution[37,38], we suggest that the reaction of AgN_3 with XN_3 (X = halogen) is a viable route to N_6 (Fig. 1b). The reactions were conducted in either a quartz tube or a U-trap by flowing gaseous Cl_2 through solid AgN_3 under reduced pressure at

[1]Institute of Organic Chemistry, Justus Liebig University Giessen, Giessen, Germany. ✉e-mail: artur.mardyukov@org.chemie.uni-giessen.de; prs@uni-giessen.de

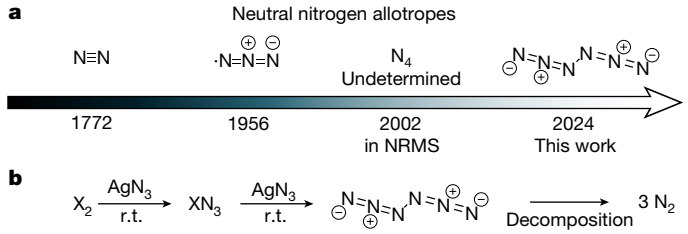

Fig. 1 | All known neutral molecular nitrogen allotropes and preparation of N_6. a, Discovery timeline (year given), composition and structure (the structure of N_4 has not been determined). **b**, Reaction sequence used in this study. r.t., room temperature.

room temperature (see the 'Synthesis details' section in Methods and Supplementary Fig. 1). Apart from the known bands of ClN_3 (ref. 39) and HN_3 (ref. 40), a distinct group of bands at 2,076.6, 2,049.0, 1,177.6 and 642.1 cm^{-1} was recorded (Supplementary Fig. 2). After irradiating the matrices with 436 nm light (Fig. 2a middle trace and Supplementary Fig. 3), all bands vanish. However, the rates of decomposition of the newly observed infrared bands differ from those attributed to ClN_3 (Supplementary Figs. 4 and 5). There were no discernible products other than chloronitrene (ClN) detected in the difference spectrum after irradiation. Furthermore, identical bands were detected when Br_2 was used instead of Cl_2, indicating that the unidentified species does not contain halogens (Fig. 2a upper trace and Supplementary Fig. 6). Also, BrN_3 does not decompose on 436 nm irradiation, providing clean decomposition spectra of the yet unidentified species.

The intensive vibrational band at 2,076.6 cm^{-1} compares favourably with the asymmetric stretching band of the azide moiety in isoelectronic N_3–NCO (2,099.1 cm^{-1}, Ar matrix)[41]. Compared with the computed harmonic vibrations at CCSD(T)/cc-pVTZ, the four bands noted above could be attributed to N_6, except the band at 2,049.0 cm^{-1} of moderate intensity, although it disappeared together with the other bands following photolysis (Supplementary Figs. 4 and 7). To determine the origin of the band at 2,049.0 cm^{-1}, anharmonic vibrational frequencies were computed at B3LYP/def2-TZVP (Supplementary Table 1). This analysis indicates that this band derives from a combination of fundamentals ν_8 (a_g symmetric N^3N^4 stretching mode) and ν_9 (b_u asymmetric $N^3N^2N^1$ stretching mode). The substantial anharmonic intensity

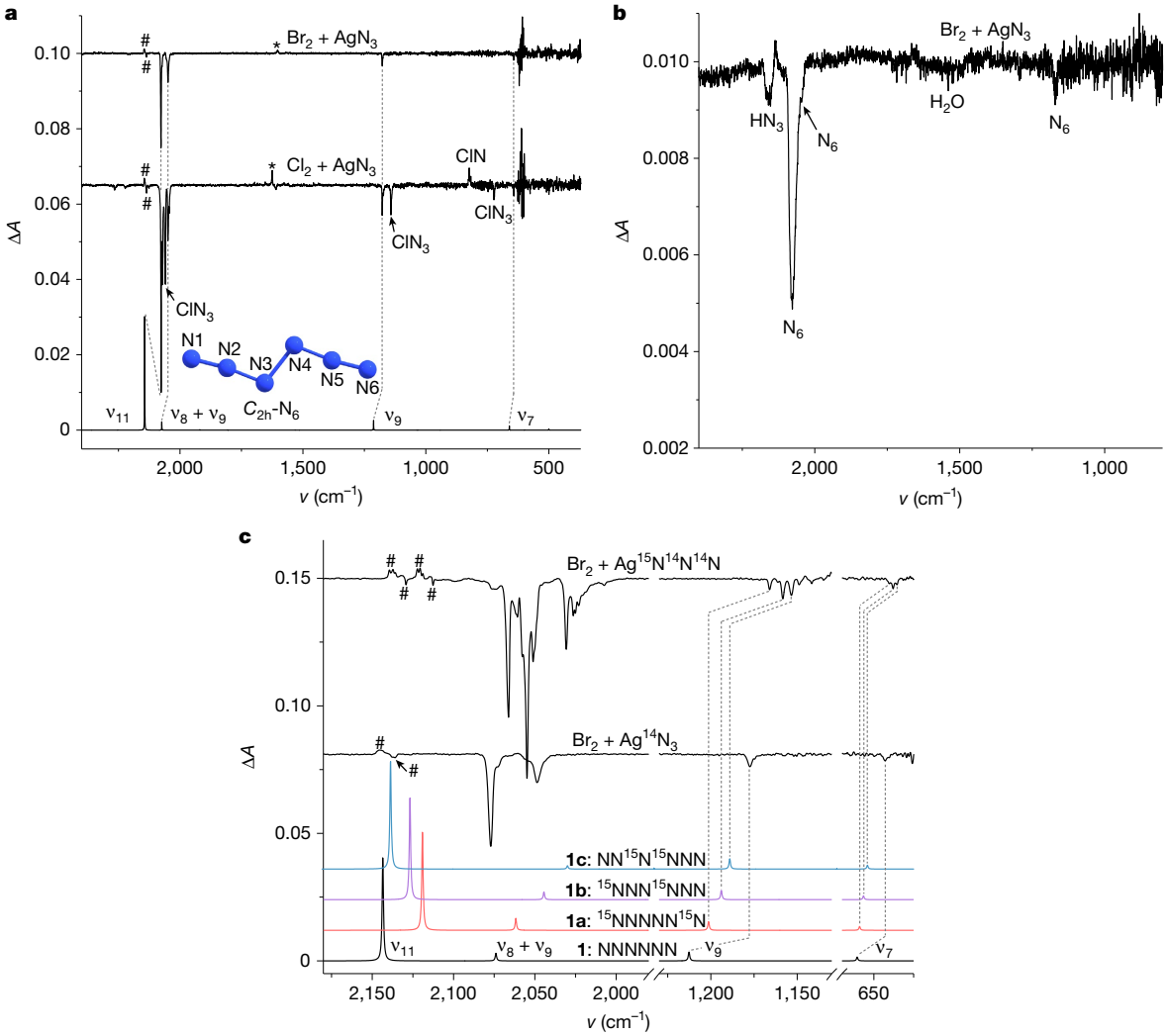

Fig. 2 | Infrared spectra of N_6 isotopomers and side products. a, Lower trace: computed anharmonic infrared spectrum of N_6 at B3LYP/def2-TZVP, including the $\nu_8 + \nu_9$ combination. Middle trace: difference spectrum showing the changes after 8 min of 436 nm irradiation of the products of the reaction of Cl_2 with AgN_3. Upper trace: difference spectrum showing the changes after 6 min of 436 nm irradiation of the reaction products of Br_2 with AgN_3. **b**, Difference spectrum of a neat N_6 film at 77 K showing the changes after 8 min of 436 nm irradiation. **c**, Bottom to top traces: computed anharmonic infrared spectrum of N_6, $^{15}NNNNN^{15}N$ (**1a**), $^{15}NNN^{15}NNN$ (**1b**) and $NN^{15}N^{15}NNN$ (**1c**) at B3LYP/def2-TZVP, including the $\nu_8 + \nu_9$ combination; difference spectrum showing the changes after 8 min of 436 nm irradiation of the reaction products of Br_2 with AgN_3; difference spectrum showing changes after 8 min of 436 nm irradiation of the reaction products of Br_2 with $Ag^{15}N^{14}N^{14}N$. Matrix sites from natural abundance and isotope-labelled HN_3 (#) and H_2O (*) are marked.

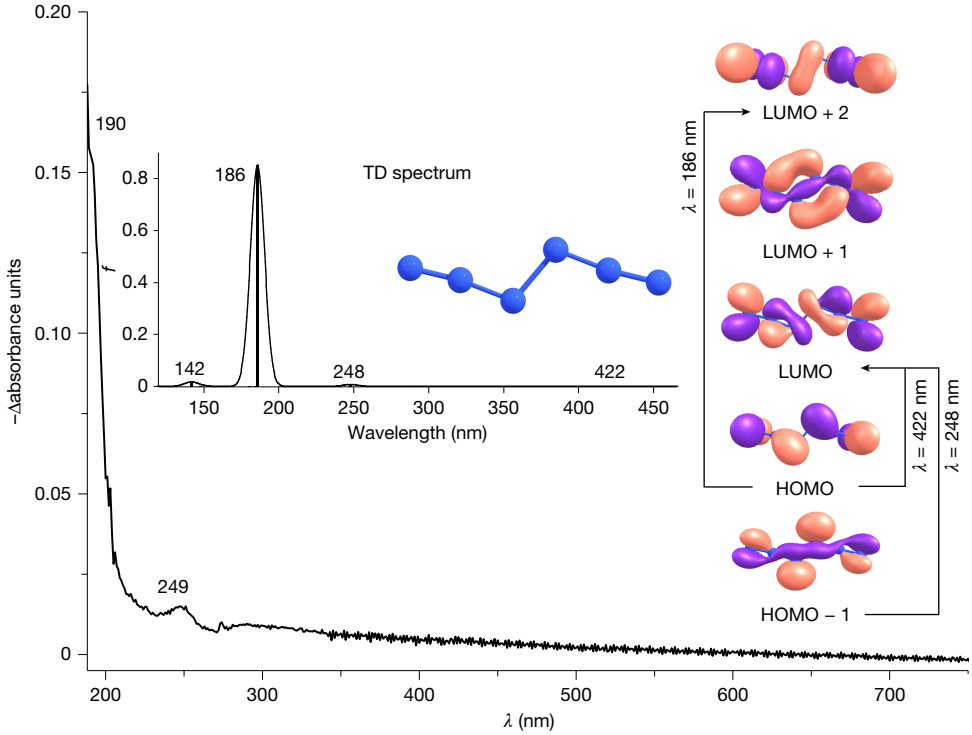

Fig. 3 | Measured and computed UV-Vis spectrum of N_6 and molecular orbitals involved in the electronic transitions. Experimental difference UV-Vis spectrum reflecting changes following 4 min of 436 nm irradiation of the reaction products of Br_2 with AgN_3 in argon at 10 K. Inset, computed [TD-B3LYP/def2-TZVP] electronic transitions for N_6 and molecular orbitals involved.

contribution (219 km mol^{-1}; Supplementary Table 2) of the fundamental ν_{11} at 2,143.5 cm^{-1} and the $\nu_8 + \nu_9$ combination is notably stronger than its fundamentals, suggesting that the combination $\nu_8 + \nu_9$ gains energy through Fermi resonance from the adjacent strong fundamental ν_{11} (ref. 41).

To confirm our assignments, isotope-labelling experiments were conducted using $Ag^{15}N^{14}N^{14}N$. Three groups of distinct peaks can be discerned in the infrared spectra (Fig. 2c and Supplementary Fig. 8), indicating the presence of two N_3 moieties in the molecule, which can be attributed to three types of isotopomer (**1a**: ^{15}NNNNN^{15}N, **1b**: ^{15}NNN^{15}NNN, **1c**: NN^{15}N^{15}NNN), respectively. In particular, the unsymmetric isotopic substitutions in **1b** lower its point group from C_{2h} to C_s. Computations delineate that the terminal (N^1 or N^6) and internal (N^3 or N^4) ^{15}N substitutions mainly influence the terminal (ν_{11}) and internal asymmetric stretching vibration (ν_9) of the N_3 moieties, respectively. This leads to a redshift of the $\nu_8 + \nu_9$ combination and a blueshift of the ν_{11} fundamental in going from **1a** to **1c**, resulting in their gradual separation. The intensity ratio of the $\nu_8 + \nu_9$ combination and the ν_{11} fundamental in **1a** is nearly 1:1, which is much higher than that in **1c** (about 1:17). These findings align well with the anharmonic infrared intensities computed by density functional theory (Supplementary Table 3), which are attributed to the closer proximity of the $\nu_8 + \nu_9$ combination to the strong ν_{11} fundamental in **1a**, resulting in an increase of the Fermi resonance and vice versa in **1c**. Statistically, the anticipated ratio of the three isotopomers should be **1a**:**1b**:**1c** = 1:2:1, which is reflected in the observed fundamental ν_7 in the experimental spectrum (Fig. 3). Furthermore, the computed intensity of ν_9 in **1c** (107 km mol^{-1}; Supplementary Table 3) is higher than that in **1a** (92 km mol^{-1}) and **1b** (98 km mol^{-1}), which matches the intensity ratios of ν_9 observed in **1a** and **1b** (approximately 1:2). The experimentally observed intensities agree with these findings and show a slightly higher intensity of ν_9 in **1c** than in **1a**.

To explore the intrinsic stability of N_6, we also prepared neat N_6 at room temperature and condensed it at liquid nitrogen temperature (77 K) as a film on the surface of the matrix window without using argon as a host gas. Irradiation of such N_6 films resulted in very similar spectral changes as those observed in argon matrices at 10 K (Fig. 2b and Supplementary Fig. 9). That is, neat N_6 is sufficiently stable at the temperature of liquid nitrogen to allow its direct identification.

Further evidence is provided by the UV-Vis spectrum of N_6. After 6 min of 436 nm irradiation of the reaction products of Br_2 with AgN_3, we observed the disappearance of the transitions at 190 and 249 nm and, consistent with the infrared experiments, no new transitions appeared (Fig. 3). All transitions correlate well with the values for the electronic excitations of N_6 at 186 nm (f = 0.8512) and 248 nm (f = 0.0078) computed at [TD-B3LYP/def2-TZVP]. Furthermore, the computations reveal a weak electronic excitation at 422 nm (f = 0.0004), corresponding to a $\pi \rightarrow \pi^*$ transition, which aligns well with the observed photochemistry.

Computations

To better understand the structure and the potential energy landscape of N_6, we computed its energy profile at CCSD(T)/cc-pVTZ (Fig. 4a (ΔG_{298K}) and Supplementary Fig. 10 (ΔH_0); see the 'Computational details' section in Methods). Only the C_{2h}-N_6 *trans*-conformer is a local minimum; the C_{2v}-N_6 *cis*-conformer is a higher-order stationary point and chemically not relevant[42,43]. The formal double bond lengths in the N_3 moieties are much longer than the triple bond in N_2 (theor. 1.104 Å; expt. 1.098 Å)[44], indicating double-bond character. Indeed, the computed $N^2 = N^3/N^4 = N^5$ bond length (1.251 Å) is close to that of *trans*-diazene (HN = NH, theor. 1.253 Å; expt. 1.252 Å)[45]. The structure of N_6 is different from the azide radical (•N = N = N, theor. 1.183 Å; expt. 1.181 Å)[46] but comparable with the N_3 moiety in hydrazoic acid (HN_3, theor. 1.247 and 1.136 Å; expt. 1.237 and 1.133 Å for the $N^1 = N^2$ and $N^2 = N^3$ bonds, respectively). The N^3–N^4 bond in N_6 (1.460 Å) compares favourably with that in hydrazine (H_2N–NH_2, theor. 1.445 Å; expt. 1.446 Å). This geometric analysis is well captured by the Lewis structure of N_6 (Fig. 1). These conclusions are supported by natural bond orbital computations, which indicate that the terminal nitrogen atoms are electronically

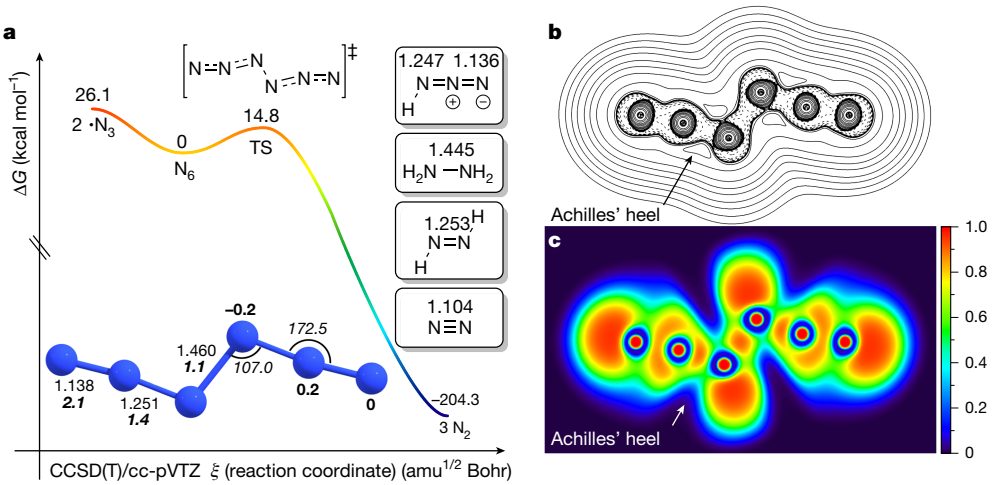

Fig. 4 | Computational analyses for N_6. a, Potential energy profile (ΔG_{298K}, kcal mol^{-1}) for N_6 at CCSD(T)/cc-pVTZ. The optimized parameters of N_6 are given in Ångstrom (normal font), degrees (italics), natural charges in bold and natural bond orders in bold italics. Insets, computed NN bond lengths for N_2, *trans*-HNNH, hydrazine and HN_3 at CCSD(T)/cc-pVTZ. **b**, Contour line map of the Laplacian of the electron density of N_6; solid and dashed lines represent positive and negative regions, respectively. **c**, ELF map.

neutral, whereas small positive and negative charges are located at N^2 and N^5 (+0.2*e*) as well as on N^3 and N^4 (−0.2*e*), respectively (Fig. 4a). Equally, N^1–N^2/N^5-N^6 have the highest bond order (2.1), followed by N^2–N^3/N^4–N^5 (1.4) and N^3–N^4 (1.1).

We visualized the Laplacian of the electron density to gauge where the bonds in N_6 are likely to break (Fig. 4b) and why the computed barrier for decomposition into three moles of N_2 is, compared with other systems, rather high ($\Delta G^{\ddagger}_{298K}$ = 14.8 kcal mol^{-1}). This barrier implies appreciable kinetic stability that is mirrored by our observations. For comparison, the computed barrier of hypothetical D_{2h}-N_4 dissociating into two N_2 is 6.5 kcal mol^{-1} at MR-AQCC/VTZ[47]. With the electron density analysis, the 'Achilles' heel' was discerned at the N^2–N^3/N^4–N^5 bonds, as evident from the vertex of positive Laplacian of the in-plane electron density. This is confirmed by the electron localization function (ELF) analysis[48] (Fig. 4c). Both the Laplacian of the electron density and the ELF analysis indicate the electron density minimum around the N^2–N^3/N^4–N^5 bonds. Hence, even though the Lewis structure would indicate N_6 breaking into two •N_3 radicals, that is, breaking of the central N^3–N^4 single bond, the computed barrier for this process amounts to sizeable ΔG_{298K} = 26.1 kcal mol^{-1} and is unproductive.

On the other hand, $\Delta G^{\ddagger}_{298K}$ for the elementary decomposition into three N_2 is 14.8 kcal mol^{-1}, implying a finite lifetime of N_6 at room temperature. As N_6 decomposition may be accelerated by QMT[21,22,49], we used canonical variational theory and small-curvature tunnelling computations at B3LYP/def2-TZVP that reveal that N_6, unlike hexazine (*cyc*-N_6)[21], is unlikely to decompose through QMT, with an estimated half-life of N_6 of more than 132 years at 77 K (Supplementary Table 4). At 298 K, the computed half-life still amounts to 35.7 ms. This supports our finding that N_6 exists long enough in the gas phase at ambient temperature to be trapped subsequently in cryogenic matrices.

According to CCSD(T)/cc-pVTZ (ΔH_0) computations, the decomposition of N_6 into three N_2 is exothermic (ΔH_0) by 185.2 kcal mol^{-1}, which is 2.2 and 1.9 times higher than the decomposition enthalpies of TNT (2,4,6-trinitrotoluene) and HMX (1,3,5,7-tetranitro-1,3,5,7-tetrazocane, octogen) by weight[50] (see the 'Computational details' section in Methods).

We report here the facile synthesis and spectroscopic identification of experimentally unreported hexanitrogen N_6. This represents the first, to our knowledge, experimentally realized neutral molecular nitrogen allotrope beyond N_2 that exhibits unexpected stability. This discovery challenges the long-held belief of the elusiveness of neutral molecular nitrogen allotropes.

Online content

Any methods, additional references, Nature Portfolio reporting summaries, source data, extended data, supplementary information, acknowledgements, peer review information; details of author contributions and competing interests; and statements of data and code availability are available at https://doi.org/10.1038/s41586-025-09032-9.

1. Christe, K. O. Polynitrogen chemistry enters the ring. *Science* **355**, 351–351 (2017).
2. Wang, Y. et al. Stabilization of hexazine rings in potassium polynitride at high pressure. *Nat. Chem.* **14**, 794–800 (2022).
3. Ninet, S. Benzene-like N_6 hexazine rings. *Nat. Chem.* **15**, 595–596 (2023).
4. Yao, Y. & Adeniyi, A. O. Solid nitrogen and nitrogen-rich compounds as high-energy-density materials. *Phys. Status Solidi B* **258**, 2000588 (2021).
5. Klapötke, T. M. & Witkowski, T. G. Nitrogen-rich energetic 1,2,5-oxadiazole-tetrazole-based energetic materials. *Propellants Explos. Pyrotech.* **40**, 366–373 (2015).
6. Nguyen, M. T. Polynitrogen compounds: 1. Structure and stability of N_4 and N_5 systems. *Coord. Chem. Rev.* **244**, 93–113 (2003).
7. Zarko, V. E. Searching for ways to create energetic materials based on polynitrogen compounds (review). *Combust. Explos. Shock Waves* **46**, 121–131 (2010).
8. Larson, Å., Larsson, M. & Östmark, H. Theoretical study of rectangular (D_{2h}) N_4. *J. Chem. Soc. Faraday Trans.* **93**, 2963–2966 (1997).
9. Glukhovtsev, M. N. & von Ragué Schleyer, P. Structures, bonding and energies of N_6 isomers. *Chem. Phys. Lett.* **198**, 547–554 (1992).
10. Glukhovtsev, M. N., Jiao, H. & von Ragué Schleyer, P. Besides N_2, what is the most stable molecule composed only of nitrogen atoms? *Inorg. Chem.* **35**, 7124–7133 (1996).
11. Strout, D. L. Acyclic N_{10} fails as a high energy density material. *J. Phys. Chem. A* **106**, 816–818 (2002).
12. Hirshberg, B., Gerber, R. B. & Krylov, A. I. Calculations predict a stable molecular crystal of N_8. *Nat. Chem.* **6**, 52–56 (2014).
13. Strout, D. L. Cage isomers of N_{14} and N_{16}: nitrogen molecules that are not a multiple of six. *J. Phys. Chem. A* **108**, 10911–10916 (2004).
14. Samartzis, P. C. & Wodtke, A. M. All-nitrogen chemistry: how far are we from N_{60}? *Int. Rev. Phys. Chem.* **25**, 527–552 (2010).
15. Mikhailov, O. V. Molecular and electronic structures of neutral polynitrogens: review on the theory and experiment in 21st century. *Int. J. Mol. Sci.* **23**, 2841 (2022).
16. Thrush, B. A. & Norrish, R. G. W. The detection of free radicals in the high intensity photolysis of hydrogen azide. *Proc. R. Soc. Lond. A* **235**, 143–147 (1956).
17. Beaman, R. A., Nelson, T., Richards, D. S. & Setser, D. W. Observation of azido radical by laser-induced fluorescence. *J. Phys. Chem.* **91**, 6090–6092 (1987).
18. Cacace, F., de Petris, G. & Troiani, A. Experimental detection of tetranitrogen. *Science* **295**, 480–481 (2002).
19. Hayon, E. & Simic, M. Absorption spectra and kinetics of the intermediate produced from the decay of azide radicals. *J. Am. Chem. Soc.* **92**, 7486–7487 (1970).
20. Zhou, H., Wong, N.-B., Zhou, G. & Tian, A. Theoretical study on "multilayer" nitrogen cages. *J. Phys. Chem. A* **110**, 3845–3852 (2006).
21. Sedgi, I. & Kozuch, S. Quantum tunneling instability of the mythical hexazine and pentazine. *Chem. Commun.* **60**, 2038–2041 (2024).
22. Schreiner, P. R. Quantum mechanical tunneling is essential to understanding chemical reactivity. *Trends Chem.* **2**, 980–989 (2020).
23. Christe, K. O., Wilson, W. W., Sheehy, J. A. & Boatz, J. A. N_5^+: a novel homoleptic polynitrogen ion as a high energy density material. *Angew. Chem. Int. Ed.* **38**, 2004–2009 (1999).

24. Vij, A. et al. Polynitrogen chemistry. Synthesis, characterization, and crystal structure of surprisingly stable fluoroantimonate salts of N_5^+. *J. Am. Chem. Soc.* **123**, 6308–6313 (2001).
25. Vij, A., Pavlovich, J. G., Wilson, W. W., Vij, V. & Christe, K. O. Experimental detection of the pentaazacyclopentadienide (pentazolate) anion, *cyclo*-N_5^-. *Angew. Chem. Int. Ed.* **41**, 3051–3054 (2002).
26. Östmark, H. et al. Detection of pentazolate anion (*cyclo*-N_5^-) from laser ionization and decomposition of solid *p*-dimethylaminophenylpentazole. *Chem. Phys. Lett.* **379**, 539–546 (2003).
27. Zhang, C. et al. Synthesis and characterization of the pentazolate anion cyclo-N_5^- in $(N_5)_6(H_3O)_3(NH_4)_4Cl$. *Science* **355**, 374–376 (2017).
28. Xu, Y. et al. A series of energetic metal pentazolate hydrates. *Nature* **549**, 78–81 (2017).
29. Xu, Y., Tian, L., Li, D., Wang, P. & Lu, M. A series of energetic *cyclo*-pentazolate salts: rapid synthesis, characterization, and promising performance. *J. Mater. Chem. A* **7**, 12468–12479 (2019).
30. Eremets, M. I., Gavriliuk, A. G., Trojan, I. A., Dzivenko, D. A. & Boehler, R. Single-bonded cubic form of nitrogen. *Nat. Mater.* **3**, 558–563 (2004).
31. Benchafia, E. M. et al. Cubic gauche polymeric nitrogen under ambient conditions. *Nat. Commun.* **8**, 930 (2017).
32. Laniel, D. et al. Aromatic hexazine $[N_6]^{4-}$ anion featured in the complex structure of the high-pressure potassium nitrogen compound K_9N_{56}. *Nat. Chem.* **15**, 641–646 (2023).
33. Greschner, M. J. et al. A new allotrope of nitrogen as high-energy density material. *J. Phys. Chem. A* **120**, 2920–2925 (2016).
34. Qian, W. Y., Mardyukov, A. & Schreiner, P. R. Hexanitrogen (N_6): a synthetic leap towards neutral nitrogen allotropes. Preprint at https://doi.org/10.26434/chemrxiv-2024-90vvx (2024).
35. Zeng, X. et al. Reaction of AgN_3 with $SOCl_2$: evidence for the formation of thionyl azide, $SO(N_3)_2$. *Inorg. Chem.* **43**, 4799–4801 (2004).
36. Raschig, F. Über Chlorazid N_3Cl. *Ber. Dtsch. Chem. Ges.* **41**, 4194–4195 (1908).
37. Lyhs, B., Bläser, D., Wölper, C., Schulz, S. & Jansen, G. A comparison of the solid-state structures of halogen azides XN_3 (X=Cl, Br, I). *Angew. Chem. Int. Ed.* **51**, 12859–12863 (2012).
38. Buzek, P., Klapötke, T. M., von Ragué Schleyer, P., Tornieporth-Oetting, I. C. & White, P. S. Iodine azide. *Angew. Chem. Int. Ed.* **32**, 275–277 (1993).
39. Shurvell, H. F. & Hyslop, D. W. Infrared spectrum of cyanogen azide. *J. Chem. Phys.* **52**, 881–887 (1970).
40. Pimental, G. C. & Charles, S. W. Infrared spectral perturbations in matrix experiments. *Pure Appl. Chem.* **7**, 111–124 (1963).
41. Zeng, X., Beckers, H. & Willner, H. Matrix isolation of two isomers of N_4CO. *Angew. Chem. Int. Ed. Engl.* **50**, 482–485 (2011).
42. Tobita, M. & Bartlett, R. J. Structure and stability of N_6 isomers and their spectroscopic characteristics. *J. Phys. Chem. A* **105**, 4107–4113 (2001).
43. Gagliardi, L., Evangelisti, S., Barone, V. & Roos, B. O. On the dissociation of N_6 into 3 N_2 molecules. *Chem. Phys. Lett.* **320**, 518–522 (2000).
44. Huber, K. P. & Herzberg, G. in *Molecular Spectra and Molecular Structure* (eds Huber, K. P. & Herzberg, G.) Ch. 2, 8–689 (Springer, 1979).
45. Carlotti, M., Johns, J. W. C. & Trombetti, A. The ν_5 fundamental bands of N_2H_2 and N_2D_2. *Can. J. Phys.* **52**, 340–344 (1974).
46. Brazier, C. R., Bernath, P. F., Burkholder, J. B. & Howard, C. J. Fourier transform spectroscopy of the ν_3 band of the N_3 radical. *J. Chem. Phys.* **89**, 1762–1767 (1988).
47. Bittererová, M., Östmark, H. & Brinck, T. Ab initio study of the ground state and the first excited state of the rectangular $(D_{2h})N_4$ molecule. *Chem. Phys. Lett.* **347**, 220–228 (2001).
48. Lu, T. & Chen, F. Multiwfn: a multifunctional wavefunction analyzer. *J. Comput. Chem.* **33**, 580–592 (2012).
49. Schreiner, P. R. Tunneling control of chemical reactions: the third reactivity paradigm. *J. Am. Chem. Soc.* **139**, 15276–15283 (2017).
50. Weggel, D. C. in *Blast Protection of Civil Infrastructures and Vehicles Using Composites* (ed. Uddin, N.) 3–43 (Woodhead Publishing, 2010).

Methods

Matrix apparatus design

For the matrix isolation studies, we used an APD Cryogenics HC-2 cryostat with a closed-cycle refrigerator system, equipped with an inner CsI window for infrared measurements. Spectra were recorded at the temperature of the matrix (10 K) with a Bruker VERTEX 70 FT-IR spectrometer with a spectral range of 4,000–400 cm^{-1} and a resolution of 0.7 cm^{-1} and UV-Vis spectra were recorded with a Jasco V-670 spectrophotometer equipped with an inner sapphire window. A high-pressure mercury lamp (HBO 200, Osram) with a monochromator (Bausch & Lomb) was used for irradiation. Cl_2 or Br_2 was evaporated (Cl_2-CCl_4: −140 °C, Br_2: −85 °C) from a storage bulb into the quartz tube or U-trap. Although not directly measured, all reaction products were co-condensed with a large excess of argon (typically 60–120 mbar from a 2,000-ml storage bulb) onto the surface of the matrix window at 10 K in several milliseconds.

Synthesis details

Warning! Silver azide and halogen azides are extremely hazardous and explosive. Such compounds should be handled with utmost care and only in very small quantities (<5 mmol). Appropriate safety precautions (blast screens, face shields, Kevlar gloves, soundproof earmuffs and protective leather clothing) are necessary. Make sure to eliminate static electricity before handling. It is also crucial to avoid friction and light exposure and prevent any contact with metals during sample handling to ensure safety.

Silver azide was synthesized by adding a stoichiometric amount of a silver nitrate–water solution to a sodium azide–water solution in the dark. The precipitate was washed three times with anhydrous ethanol. The resulting slurry was loosely dispersed on one side of the inner surface of a straight quartz tube (ø 10 × 1) or the inner surface of a U-trap (inside diameter 10 mm) and then brought to reduced pressure to remove the solvent. Typically, 0.6 mmol and 2.5 mmol of AgN_3 are required for the straight quartz tube and U-trap, respectively. $Na^{15}N^{14}N^{14}N$ (>99% ^{15}N, Sigma-Aldridge) was used for isotope labelling experiments. Chlorine gas was bubbled into CCl_4 at 0 °C and degassed before use. Bromine was purified by vacuum distillation before use. Typically, 3 mmol of halogen were stored in the storage bulb for the reaction.

Computational details

Geometry optimizations and energy computations were carried out at the CCSD(T)/cc-pVTZ[51–53] levels of theory using ORCA 5.0 (with keywords verytightscf and verytightopt)[54]. B3LYP[55,56] computations (geometry optimizations, energy computations (all free energies were computed at 298 K), harmonic vibrational analysis and DVPT2 anharmonic vibrational analysis) were performed using Gaussian 16 (ref. 57) with a def2-TZVP basis set[58]. Local minima were confirmed by vibrational frequencies analyses and transition states were further confirmed by intrinsic reaction coordinate computations. Harmonic vibrational analysis at CCSD(T)/cc-pVTZ was performed using CFOUR v2.1 (ref. 59). Wavefunction analysis (Laplacian of electron density and electron localization function) results were obtained from Multiwfn 3.8 (ref. 60) at CCSD(T)/cc-pVTZ. Natural bond order analysis and resonance structures were computed with NBO 7.0 (refs. 61,62). CVT/SCT (canonical variational transition state theory with small-curvature tunnelling) and CVT/ZCT (canonical variational transition state theory with zero-curvature tunnelling) computations were carried out with Gaussrate 17 (refs. 27,63–67) as an interface between Gaussian 16 and Polyrate[68]. Furthermore, local stretching force constants were obtained by LModeA-nano[69] as a plugin of the open-source version of the visualization program PyMOL.

Detonation calculation details

First, the density (ρ, in cm^3 per molecule) of the N_6 crystal was determined using electrostatic interaction correction as suggested by Politzer et al.[70] (equation (2)). M_m (84.04/(6.02 × 10^{23}) g per molecule) is the molecular mass. V_m (610.52/(1.89 × 10^8)^3 cm^3 per molecule) is the volume of the isolated gas-phase molecule, which was determined by the 0.001 a.u. density envelope using the marching tetrahedron method[60,71]. ν is the parameter of balance between positive and negative surface potentials[72] (equation (2)). σ_{tot}^2 (48.40 kcal^2 mol^{-2}) is the strengths and variabilities of the overall surface potentials, which could be derived from variance of positive (σ_+^2, 31.06 kcal^2 mol^{-2}) and negative charges (σ_-^2, 17.34 kcal^2 mol^{-2}) with equation (3). α (0.9183), β (0.0028) and γ (0.0443) are coefficients.

$$\rho = \alpha\left(\frac{M_m}{V_m}\right) + \beta(\nu\sigma_{tot}^2) + \gamma \quad (1)$$

$$\nu = \frac{\sigma_+^2\sigma_-^2}{(\sigma_+^2 + \sigma_-^2)^2} \quad (2)$$

$$\sigma_{tot}^2 = \sigma_+^2 + \sigma_-^2 \quad (3)$$

The detonation velocity (D) and detonation pressure (P) were calculated using the Kamlet–Jacobs equation[73] (equations (4) and (5)). N is the number of moles of the gas generated per gram (equation (6)), $\overline{M}$ is the average molecular weight of the gaseous product (equation (7)), Q is the heat of detonation (equation (8)), M is the molecular weight (84.04 g mol^{-1}), ΔH_f is the standard heat of formation (774.88 kJ mol^{-1}, which was derived from the energy difference of the computed enthalpy at 298 K between C_{2h}-N_6 and 3 moles of N_2) and a (0), b (0), c (0) and d (6) represent the number of C, H, O, and N atoms in the molecule, respectively.

$$D = 1.01\left(N\sqrt{\overline{M}Q}\right)^{\frac{1}{2}}(1 + 1.3\rho) \quad (4)$$

$$P = 1.558\rho^2 N\sqrt{\overline{M}Q} \quad (5)$$

$$N = \frac{b + 2c + 2d}{4M} \quad (6)$$

$$\overline{M} = \frac{4M}{b + 2c + 2d} \quad (7)$$

$$Q = \frac{28.9b + 94.05a + 0.239\Delta H_f}{M} \quad (8)$$

Assessing the energetic performance using the Kamlet–Jacobs equation[73], the CCSD(T)/cc-pVTZ level of theory predicts a lower density (ρ: 1.51 g cm^{-3}) than that of TNT (1.65 g cm^{-3}) and an excellent detonation performance (detonation velocity D: 8,930 m s^{-1}; detonation pressure P: 31.7 GPa). This compares favourably with several well-known explosives, for example, TNT (D: 6,900 m s^{-1}; P: 21.0 GPa), RDX (1,3,5-trinitro-1,3,5-triazinane; D: 8,750 m s^{-1}; P: 34.5 GPa) and FOX-7 (1,1-diamino-2,2-dinitroethylene; D: 8,870 m s^{-1}; P: 34.5 GPa)[74].

Energy-releasing equivalent calculation details

A kiloton of N_6 is 1.19 × 10^7 mol, which can release an energy of 2.20 × 10^9 kcal (9.21 terajoules) based on the enthalpy (ΔH_0). Considering that the standard kiloton TNT equivalent is 4.184 terajoules, N_6 can release 2.2 times the energy of TNT of the same weight. On the basis of the documented TNT equivalent based on weight for HMX (1.15) and RDX (1.15)[50], N_6 can release 1.9 times the energy of HMX or RDX with the same weight.

51. Pople, J. A., Head-Gordon, M. & Raghavachari, K. Quadratic configuration interaction. A general technique for determining electron correlation energies. *J. Chem. Phys.* **87**, 5968–5975 (1987).

52. Bartlett, R. J. & Purvis, G. D. Many-body perturbation theory, coupled-pair many-electron theory, and the importance of quadruple excitations for the correlation problem. *Int. J. Mol. Sci.* **14**, 561–581 (1978).
53. Pople, J. A., Krishnan, R., Schlegel, H. B. & Binkley, J. S. Electron correlation theories and their application to the study of simple reaction potential surfaces. *Int. J. Mol. Sci.* **14**, 545–560 (1978).
54. Neese, F. Software update: the ORCA program system—version 5.0. *WIREs Comput. Mol. Sci.* **12**, e1606 (2022).
55. Becke, A. D. Density-functional thermochemistry. III. The role of exact exchange. *J. Chem. Phys.* **98**, 5648–5652 (1993).
56. Stephens, P. J., Devlin, F. J., Chabalowski, C. F. & Frisch, M. J. Ab initio calculation of vibrational absorption and circular dichroism spectra using density functional force fields. *J. Phys. Chem.* **98**, 11623–11627 (1994).
57. Frisch, M. J. et al. Gaussian 16, Revision B.01 (Gaussian, Inc., 2016).
58. Weigend, F. & Ahlrichs, R. Balanced basis sets of split valence, triple zeta valence and quadruple zeta valence quality for H to Rn: design and assessment of accuracy. *Phys. Chem. Chem. Phys.* **7**, 3297–3305 (2005).
59. Stanton, J. F. et al. CFOUR, coupled-cluster techniques for computational chemistry, a quantum-chemical program package with the integral packages MOLECULE (J. Almlöf and PR Taylor), PROPS (PR Taylor) (2014).
60. Lu, T. & Chen, F. Quantitative analysis of molecular surface based on improved Marching Tetrahedra algorithm. *J. Mol. Graph. Model.* **38**, 314–323 (2012).
61. Glendening, E. D., Landis, C. R. & Weinhold, F. NBO 7.0: new vistas in localized and delocalized chemical bonding theory. *J. Comput. Chem.* **40**, 2234–2241 (2019).
62. Glendening, E. D., Landis, C. R. & Weinhold, F. Natural bond orbital methods. *WIREs Comput. Mol. Sci.* **2**, 1–42 (2012).
63. Zheng, J. et al. *Gaussrate 17-B* (Univ. Minnesota, 2017).
64. Garrett, B. C. & Truhlar, D. G. Generalized transition state theory. Bond energy-bond order method for canonical variational calculations with application to hydrogen atom transfer reactions. *J. Am. Chem. Soc.* **101**, 4534–4548 (1979).
65. Garrett, B. C. & Truhlar, D. G. Criterion of minimum state density in the transition state theory of bimolecular reactions. *J. Chem. Phys.* **70**, 1593–1598 (1979).
66. Garrett, B. C., Truhlar, D. G., Grev, R. S. & Magnuson, A. W. Improved treatment of threshold contributions in variational transition-state theory. *J. Phys. Chem.* **84**, 1730–1748 (1980).
67. Truhlar, D. G., Issacson, A., Skodje, R. & Garrett, B. C. Additions and corrections - incorporation of quantum effects in generalized-transition-state theory. *J. Phys. Chem.* **87**, 4554–4554 (1983).
68. Zheng, J. et al. *Polyrate-version 2017-C* (Univ. Minnesota, 2017).
69. Tao, Y., Zou, W., Nanayakkara, S. & Kraka, E. LModeA-nano: a PyMOL plugin for calculating bond strength in solids, surfaces, and molecules via local vibrational mode analysis. *J. Chem. Theory Comput.* **18**, 1821–1837 (2022).
70. Politzer, P., Martinez, J., Murray, J. S., Concha, M. C. & Toro-Labbé, A. An electrostatic interaction correction for improved crystal density prediction. *Mol. Phys.* **107**, 2095–2101 (2009).
71. Bader, R. F. W., Carroll, M. T., Cheeseman, J. R. & Chang, C. Properties of atoms in molecules: atomic volumes. *J. Am. Chem. Soc.* **109**, 7968–7979 (1987).
72. Murray, J. S., Concha, M. C. & Politzer, P. Links between surface electrostatic potentials of energetic molecules, impact sensitivities and C–NO_2/N–NO_2 bond dissociation energies. *Mol. Phys.* **107**, 89–97 (2009).
73. Kamlet, M. J. & Jacobs, S. J. Chemistry of detonations. I. A simple method for calculating detonation properties of C–H–N–O explosives. *J. Chem. Phys.* **48**, 23–35 (1968).
74. Prazyan, T. L. & Zhuravlev, Y. N. Computer simulation of the structure and electronic and detonation properties of energy materials. *Combust. Explos. Shock Waves* **53**, 718–723 (2017).

Acknowledgements Financial support by the Deutsche Forschungsgemeinschaft (DFG) through grant MA 8773/3-1 (A.M.) is gratefully acknowledged. We sincerely thank X. Bi (Northeast Normal University), T. M. Klapötke (Ludwig Maximilian University of Munich) and Y. Ning (Northeast Normal University) for their valuable suggestions for the synthesis of silver azide and T. Lu (Beijing Kein Research Center for Natural Sciences) for advice about the detonation performance computations. We also thank W. D. Allen (University of Georgia) and X. Zeng (Fudan University) for carefully reading and commenting on the manuscript.

Author contributions W.Q., A.M. and P.R.S. conceived the project. W.Q. and A.M. designed and conducted the experiments, performed computations and collected all data. W.Q. wrote the original manuscript. W.Q., A.M. and P.R.S. revised the manuscript. A.M. and P.R.S. supervised the project.

Funding Open access funding provided by Justus-Liebig-Universität Gießen.

Competing interests W.Q., A.M., and P.R.S. are inventors on European patent application EP24194869 (16 August 2024), submitted by the Justus Liebig University Giessen, which covers a method for producing molecular polynitrogens.

Additional information

Supplementary information The online version contains supplementary material available at https://doi.org/10.1038/s41586-025-09032-9.

Correspondence and requests for materials should be addressed to Artur Mardyukov or Peter R. Schreiner.

Peer review information *Nature* thanks Chunlin He, Thomas Klapötke and the other, anonymous, reviewer(s) for their contribution to the peer review of this work.